Published in final edited form as:
Cell Metab. 2011 October 5; 14(4): 491–503. doi:10.1016/j.cmet.2011.08.006.

The Differential Role of *Hif1β/Arnt* and the Hypoxic Response in Adipose Function, Fibrosis, and Inflammation

Kevin Y. Lee[1], **Stephane Gesta**[1], **Jeremie Boucher**[1], **Xiaohui L. Wang**[1], and **C. Ronald Kahn**[1,*]

[1]Section on Integrative Physiology and Metabolism, Joslin Diabetes Center, Harvard Medical School, Boston, MA

Abstract

In obesity, adipocytes distant from vasculature become hypoxic and dysfunctional. This hypoxic response is mediated by hypoxia inducible factors (*Hif1α, Hif2α, and Hif3α*), and their obligate partner *Hif1β* (*Arnt)*. We show that mice lacking *Hif1β* in fat (FH1βKO) are lean, exhibit reduced adipocyte size, and are protected from age and diet-induced glucose intolerance. There is also reduced *Vegf* and vascular permeability in FH1βKO fat, but diet-induced inflammation and fibrosis is unchanged. Adipocytes from FH1βKO mice have reduced glucose uptake due to decreased *Glut1* and *Glut4*, which is mirrored in 3T3-L1 adipocytes with *Hif1β* knockdown. *Hif1β* knockdown cells also fail to respond appropriately to hypoxia with reduced cellular respiration and reduced mitochondrial gene expression. Some, but not all, of these effects are reproduced by *Hif1α* knockdown. Thus, *Hif1β/Arnt* regulates glucose uptake, mitochondrial gene expression, and vascular permeability to control adipose mass and function, providing a novel target for obesity therapy.

Keywords

Obesity; Adipocyte; Vegf; Oxidative Phosphorylation; Glucose Uptake

Introduction

Over the past 30 years the prevalence of obesity dramatically increased, along with associated diseases, including type 2 diabetes, coronary heart disease, hypertension, hepatosteotosis, and even cancer (Bray, 2004). With obesity, adipocytes distant from the vasculature become hypoxic, and this has been proposed to be an important contributor to adipose tissue dysfunction leading to insulin resistance and diabetes (Trayhurn and Wood, 2004).

The main sensor and mediator of the hypoxic response is the *Hif* family of proteins. Hifs are basic helix-loop-helix transcription factors which function as α and β heterodimers. Hif proteins are essential for normal development, and whole-body *Hif1α* and *Hif2α* knockout mice die in mid-gestation with developmental defects of the cardiovascular system (Iyer et

*To whom correspondence should be addressed: C. Ronald Kahn, MD, Obesity Section, Joslin Diabetes Center, 1 Joslin Place, Phone: (617) 732-2635, Fax: (617) 732-2593, C.Ronald.Kahn@joslin.harvard.edu .

al., 1998; Scortegagna et al., 2003; Compernolle et al., 2002). All Hif-*α* isoforms require *Hif1β* as an obligate heterodimeric partner to function as transcriptional regulators. *Hif1β* is also known as *Arnt* (the aryl hydrocarbon receptor Ahr nuclear translocator), since it acts as the transcriptional partner for the aryl hydrocarbon receptor (*Ahr*) and single-minded gene1 (*Sim1*) (Swanson et al., 1995). Ablation of *Hif1β* therefore results in an absence of *Hif*- and Ahr-induced signaling. Whole body *Hif1β* knockout mice die at mid-gestation due to numerous developmental defects (Maltepe et al., 1997). Ablation of *Hif1β* in the liver is sufficient to lead to lack of target gene induction of *Hif1α*, *Hif2α* and Ahr (Tomita et al., 2000; Rankin et al., 2005). In addition, we have previously demonstrated that type 2 diabetes subjects have lower *Hif1β* levels in both the β cells and liver contributing to impaired glucose-stimulated insulin secretion and aberrant expression of key lipogenic and gluconeogenic enzymes (Gunton et al., 2005; Wang et al., 2009).

Recently, all *Hif-α* subunits have been shown to have roles in adipocyte biology. Over-expression of constitutively active *Hif1α* in mouse adipose tissue induces fibrosis and insulin resistance (Halberg et al., 2009). Conversely, expression of a dominant negative *Hif1α* in adipose tissue perturbs brown fat function leading to increased obesity and insulin resistance (Zhang et al., 2010). *Hif2α* and *Hif3α* have both been shown to have roles in adipogenesis and adipocyte function (Peng et al., 2000; Hatanaka et al., 2009). Finally, insulin resistance is observed in 3T3-L1 adipocytes over-expressing *Hif1α* or *Hif2α* (Regazzetti et al., 2009).

In the present study, we have evaluated the role of the Hif transcriptional system by creation of a mouse lacking *Hif1β* (Arnt) in adipose tissue. We find that these mice are resistant to age and diet-induced obesity and its associated glucose intolerance. This occurs through effects on varied processes, including effects on adipocyte cell size, glucose uptake, control of vascular permeability, and regulation of the hypoxic response. The effects are mediated in part through the actions of *Hif1α*, and involve both cell autonomous and cell non-autonomous changes mediated via Vegf. Taken together, these data demonstrate a critical role for *Hif1β* in the control of adipose tissue mass and function.

Results

aP2-Cre effectively ablates *Hif1β* from adipocytes

We created mice with an ablation of *Hif1β* in adipocytes by breeding aP2-Cre transgenic mice and mice carrying a *Hif1β* allele with loxP sites surrounding exon 5 (Abel et al., 2001). *aP2-Cre*; $Hif1\beta^{f/f}$ (termed fat-specific *Hif1β* knockout or FH1βKO) mice were born at the expected ratio and exhibited no overt phenotypic abnormalities. Efficient and specific ablation of *Hif1β* was confirmed by qPCR analysis. *Hif1β* mRNA was reduced >90% reduction in isolated subcutaneous and perigonadal adipocytes from fat and brown adipose tissue from 6 to 8 week old female mice (Figure 1a). Western blot analysis of perigonadal isolated adipocytes confirmed a corresponding decrease in *Hif1β* protein levels (Figure 1b). No changes in *Hif1β* mRNA levels were observed in liver, pancreas and heart (Figure 1c). In addition, qPCR analysis of the stromovascular fraction, which contains preadipocytes, from subcutaneous but not the perigonadal adipose tissue, showed a significant 40% reduction of *Hif1β* mRNA levels (Figure 1d). No compensatory upregulation of the related gene *Arnt2* was noted (Figure 1e).

Ablation of *Hif1β* attenuates age and diet-induced obesity

FH1βKO and littermate control floxed mice were fed a standard chow diet (22% of calories as fat) or subjected to high fat diet (HFD) (60% of calories as fat) starting at 6 weeks of age. On a chow diet, both male and female FH1βKO exhibited reduced weight gain compared to controls, by 10 months of age male FH1βKO mice had a 24% reduction in weight gain,

(Figure 2a) and females FH1βKO mice were also 32% lighter (Figure S1a). Male FH1βKO also exhibited a ~16% reduction in weight gain when fed a HFD for 10 weeks compared to controls. Similar results were observed in female FH1βKO mice (Figure 2b). This weight gain difference was observed as early as eight weeks of HFD (Figure S1a).

DEXA scans of chow fed animals at 20 weeks of age showed that male and female FH1βKO mice had 31% and 55% decreases of visceral fat mass and 20% and 33% decreases in subcutaneous fat mass, respectively (Figure 2c). Histological examination of the fat pads from 6-8 wk old animals showed no changes in adipose tissue morphology. By 20 weeks of age, there was reduced lipid droplet size in subcutaneous and perigonadal adipocytes in FH1βKO mice, as well as, reduced triglyceride accumulation in the BAT (Figures 2d and S2b). Median diameters of subcutaneous and perigonadal adipocytes were decreased by 42% and 26%, respectively, in FH1βKO animals relative to controls after 20 weeks of chow diet (Figures 2e and S2b-c). Similar results were seen after 12 weeks of HFD exposure, with a ~24% decrease in median adipocyte diameter in both white fat depots (Figures 2e and S2c). Consistent with the reduced adipose tissue mass on HFD, FH1βKO female and male mice had 41% and 34% decreases in leptin levels compared to controls. No changes in serum adiponectin levels were observed (Figures S1d,e). Together, these data show that FH1βKO mice are partially protected against age and diet-induced obesity due to a decrease in the ability of adipocytes to undergo hypertrophy.

Physiological parameters in FH1βKO mice

Young (8-10 week old) FH1βKO mice had no abnormality on any measured metabolic parameter, including fasting and fed glucose, fasting and fed insulin levels, serum free fatty acids, or glucose and insulin tolerance tests (Table S1; Figure S2a). However, with aging, metabolic parameters in FH1βKO mice differed from controls. Old FH1βKO female and male mice had improved glucose tolerance with 53% and 31% reductions of area under the curve on glucose tolerance testing as compared to controls. Old male FH1βKO mice also had lower fasting glucose levels (Table S1). Likewise, after HFD challenge, male and female FH1βKO mice had a 33% reduction under the curve on glucose tolerance testing as compared to controls (Table S1; Figure S2a). The reduction in weight gain and attenuation of obesity-induced glucose intolerance in the FH1βKO mice was not associated with a change in insulin tolerance (Table S1).

Hif1β detection had no discernable effect on other metabolically important tissues. In the liver, there were no changes in lipid accumulation, as assessed by Oil Red O staining and triglyceride analysis, or histological changes between FH1βKO and control mice, even after HFD exposure (Figures S2b-c). Additionally, western blot analysis of liver extracts showed no changes in phosphorylation of IRS-1, Akt, or MAP kinase in response to insulin, suggesting no major changes in insulin sensitivity in the liver of FH1βKO mice (Figure S2d). Finally, islet function, as assessed by glucose-stimulated insulin secretion was not affected in FH1βKO mice (Figure S3e).

To better understand the basis for differences in weight gain and fat mass, indirect calorimetry was performed on young FH1βKO and controls mice. No differences were observed when animal have been fed with chow diet. However, after 10 weeks of HFD feeding, FH1βKO had a significant 11-15% increase in average oxygen consumption during both the light phase (8508 + 370 in FH1βKO versus 7417 + 398 mL/kg lean mass/hr, $p<0.05$) and dark phase of the diurnal cycle (9365 + 416 versus 8476 + 408 mL/kg lean mass/hr, $p<0.05$) (Table S2). In addition, FH1βKO consumed similar amount of calories and had comparable levels of activity as controls. Together these data suggest that the decreased weight gain exhibited by FH1βKO mice was due to increased energy expenditure.

Ablation of *Hif1β* does not affect fibrosis and macrophage infiltration

Over-expression of *Hif1α* has been reported to increase fibrosis in adipocytes (Halberg et al., 2009). In control mice, expression of known markers of fibrosis *mLox* and *Col1a1* were increased >50% and 200%, respectively, in the subcutaneous fat after 12 weeks of HFD, while *Col6a1* expression was increased by over 80% in perigonadal fat (Figures S1f-h). Similar increases in markers of fibrosis were observed in the FH1βKO mouse indicating that these effects occurred independently of Hif signaling.

Determination of the expression levels of inflammation markers in adipose tissue revealed a significant increase in pro-inflammatory cytokines tumor necrosis factor α (*Tnfα*) and macrophage chemo-attractant protein-1 (*Mcp1*) in both subcutaneous and perigonadal fat of control mice after HFD exposure (Figures S2i-j). *Mcp1* was also increased in the brown fat of control mice on HFD. Likewise, expression of macrophage marker, CD68 was significantly increased in the subcutaneous and perigonadal fat pads of control mice, and interleukin-6 (*Il6*) was significantly increased in the subcutaneous fat of control mice on HFD (Figures S2k-l). Immunohistochemical staining of the macrophage marker F4/80 in control mice showed a marked increase after HFD exposure. All of these markers of inflammation and macrophage infiltration showed almost identical increases in the fat depots of FH1βKO mice (Figures 3Si-m). Therefore, although *Hif1β* ablation leads to decreased adipose cell size, induction of makers of fibrosis and macrophage infiltration, classically observed in adipose tissue with obesity, were not reduced in FH1βKO mice after challenge with a HFD.

Hif1β ablation decreases glucose uptake

The decreased adipocyte size observed in FH1βKO mice could be the result of increased lipolysis, decreased lipogenesis, and/or a defect in adipocyte differentiation. qPCR analysis from subcutaneous and perigonadal fat of FH1βKO and littermate control animals revealed no significant differences in the mRNA levels of regulators and markers of adipogenesis, including Cebp*β*, Cebp*δ*, Ppar*γ*, FoxO1, and aP2 (Figures S3a,b) suggesting that *Hif1β* ablation does not impair adipocyte differentiation. Additionally, no differences in basal or isoproterenol-stimulated lipolysis were observed (Figure S3g). However, both basal and insulin-stimulated lipogenesis rates were markedly reduced in isolated subcutaneous (~60%) and perigonadal (~80%) adipocytes from male FH1βKO mice (Figure 3a). Likewise, in subcutaneous fat, uptake of [H^3] 2-deoxyglucose was reduced by >40% in the basal state and by 19-40% in the insulin-stimulated state in FH1βKO mice compared to controls (Figure 3b). This reduction was even greater in perigonadal adipocytes, with an 86% decrease in basal glucose uptake and 52-78% decreases in insulin-stimulated glucose uptake over the concentration range of 0.1 nM to 100 nM insulin (Figure 3b).

In agreement with these defects in adipocyte glucose uptake and lipogenesis, gene expression levels of the glucose transporter *Glut4* and *Glut1* were reduced by >50% and 24%, respectively, in both perigonadal and subcutaneous fat of 6-8 week old in FH1βKO mice (Figure 3c). Thus, ablation of *Hif1β* leads to decreased levels of glucose transport proteins, which results in decreases in glucose transport and, subsequently, decreased lipogenesis.

qPCR analysis of the key lipogenic genes, including sterol-regulatory-element-binding protein 1c (*Srebp1C*), acetyl-CoA carboxylase (*Acc1*) and fatty acid synthase (*Fas*), in fat of 6 week-old male FH1βKO males showed no changes in expression compared with controls (Figures S3c,d). After exposure to HFD for 12 weeks, qPCR analysis revealed significantly lower levels of *Srebp1C*, *Acc*1, *Fas*, and stearoyl-coenzyme A desaturase 1 (*Scd1*) mRNA in the fat depots of FH1βKO mice (Figures S3e,f).

Knockdown of *Hif1β* reduces glucose uptake

To further investigate the mechanisms underlying the effects of *Hif1β* in adipocytes, we utilized shRNA lentiviruses directed against *Hif1β* to create two independent stable 3T3-L1 knockdown cell lines, sh*Hif1β–1* and sh*Hif1β–2*, with 87 % and 93% reductions in *Hif1β* expression (Figure 4a). This decrease was specific; the highly homologous *Arnt2* was decreased by only 9% and 41% in these two cell lines, respectively (Figure 4a). Western blot analysis showed no detectible *Hif1β* protein levels in either sh*Hif1β* cell lines (Figure 4b). These sh*Hif1β* 3T3-L1 adipocyte cell lines displayed no difference in lipid accumulation, as visualized by Oil Red O staining or triglyceride quantitation (Figures S4a, 4c). No changes in the expression of the major regulators and markers of adipose differentiation, including *Pparγ*, *Cebpα*, *Cebpβ*, *Cebpβ*, *Foxo1*, and *aP2* were observed (Figure S4b). Thus, knockdown of *Hif1β* does not affect adipocyte differentiation.

However, basal and insulin-stimulated uptake of 2-deoxyglucose were decreased by 20-30% in both sh*Hif1β–1* and sh*Hif1β–2* adipocytes compared to controls (Figure 4c). This correlated with 28 and 32% decreases in *Glut1* and *Glut4* mRNA levels in sh*Hif1β–1* cells, and 45% and 21% decreases in sh*Hif1β–2* cells under normoxic conditions (Figures 4d, e).

These sh*Hif1β* knockout cells showed altered responses to hypoxia and the hypoxia mimetic $CoCl_2$. Thus, in control cells *Glut1* expression was increased approximately 7-fold by hypoxia (16 hours at 0.1% O_2) and 3-fold by following treatment with $CoCl_2$ (200 μM for 16h), whereas in sh*Hif1β* cells, the induction of *Glut1* was blunted by 47% to 60% (Figure 4d). In these cells, Western blot analysis demonstrated that $CoCl_2$ was sufficient to also strongly increased *Hif1α* protein (Figure S4d). Western blot analysis confirmed the reduced *Glut1* and *Glut4* levels in sh*Hif1β* adipocytes under normoxic conditions (Figure 4f). *Glut4* mRNA levels were not significantly changed by hypoxia or $CoCl_2$ treatment in either sh*Hif1β* or control cells, and expression levels remain significantly different between sh*Hif1β* and control adipocytes after treatment with $CoCl_2$ (Figure 4e).

As previously reported, osmotic shock can stimulate *Glut4* translocation in 3T3-L1 adipocytes in an insulin independent manner (Chen et al., 1997). sh*Hif1β* cells exhibited a decrease of ~25% in 2-deoxygucose uptake when subjected to osmotic shock with 600 mM sorbitol (Figure S4c). By contrast, no change in fatty acid uptake, measured by ^{14}C-labelled palmitic acid incorporation, was observed in sh*Hif1β* cells (Figure S4e). Thus, the decreased levels of glucose transport proteins that result in decreases in glucose transport are cell autonomous effects caused by the ablation of *Hif1β*.

Hif1β ablation decreases vascular permeability

Many tissues have been shown to undergo remodeling of vascular structure in response to hypoxia (Kaluz et al., 2008). To determine if ablation of *Hif1β* in adipocytes would cause a difference in vascular structure in fat, we visualized blood vessels using CD31 immunofluorescence in whole mount fat pads from FH1βKO and control mice. Vascular density within individual fat pads exhibited heterogeneity, but there were no significant differences in blood vessel density in either subcutaneous or perigonadal fat pads of young or HFD-exposed FH1βKO mice compared to control mice (Figure 5a, S5a). Capillary density at eight weeks of age, as assessed by immunofluorescence for GSL I-isolectin, was also unchanged in FH1βKO males (Figure S5c,d). After HFD, capillary density was increased by 31% the subcutaneous fat and several fold in brown adipose tissue of FH1βKO males (Figure 5b, S6e). However, these increases are most likely due to the difference in adipose cell size, which leads to an apparent difference in cellular density in microscopic fields between controls and FH1βKO.

Staining with pimonidazole to identify hypoxic regions in fat pads from eight-week-old mice showed similar results. Under chow diet, young FH1βKO and control animals had very little pimonidazole staining in either the subcutaneous or perigonadal adipose tissue. After HFD, areas of scattered pimonidazole positivity were found in fat pads of both FH1βKO and control mice with no apparent differences between genotypes (Figure S5b).

Eight week old FH1βKO mice exhibited no changes in body weight or fat pad weight compared to controls. However, at this age, extravasation of Evans Blue dye into the subcutaneous and perigonadal fat pads revealed a ~40% reduction in vascular permeability in adipose tissue of FH1βKO mice (Figure 5c, S5f). Thus, FH1βKO mice do not have reduced vasculature, but do have a significant reduction in vascular permeability in fat.

Changes in vascular permeability during hypoxia are primarily mediated by vascular endothelial growth factor (*Vegf*). In all fat depots of FH1βKO mice *Vegf* mRNA expression was decreased by 40%, and this was confirmed by a corresponding decrease in Vegf protein level in isolated adipocytes from perigonadal fat (Figure 5c). Likewise, *Vegf* mRNA levels were decreased by 37% in both sh*Hif1β* knockdown cell lines under normoxic conditions (Figure 5e). In both control and knockdown cell lines, hypoxia led to a 3-fold increase in *Vegf* mRNA although *Vegf* expression remained proportionately lower in the sh*Hif1β* cells. These results were confirmed by western blot analysis of Vegf protein from whole cell lysates and surrounding tissue culture media (Figure 5f) mirroring the *in vivo* finding that loss of *Hif1β* leads to a decrease in *Vegf* and vascular permeability.

Role of *Hif1β* in hypoxia sensing

To assess the consequences of *Hif1β* ablation on cellular respiration, we used a Seahorse extracellular flux analyzer to determine basal and maximal mitochondrial respiration, ATP turnover, and non-mitochondrial respiration by measuring oxygen consumption rate (OCR) of differentiated control and *Hif1β* knockdown 3T3-L1 cells. Under normoxic conditions, no significant differences were seen in the bioenergetics profiles of control and sh*Hif1β* 3T3-L1 adipocytes (Figure 6a). Pretreatment of the control cells for 16 hrs with the hypoxia mimetic $CoCl_2$ (200 μM) led to a ~33% reduction of basal respiration and a striking 67% reduction in maximal respiratory capacity. By comparison, sh*Hif1β* 3T3-L1 adipocytes showed no decrease in basal or maximal respiration after $CoCl_2$ treatment (Figure 6a-c). No significant differences were found between control and knockdown cells in the proton leak or non-mitochondrial respiration. In order to investigate the molecular mechanisms that are changed in hypoxia sensing in the sh*Hif1β* cells, we performed qPCR analysis on genes encoding mitochondrial proteins involved in oxidative phosphorylation. Numerous genes were unchanged by *Hif1β* ablation either in normoxic conditions or after pre-treatment with $CoCl_2$ (Figures S7a,b). Likewise, under normoxic conditions, no changes were observed in cytochrome c1 (*Cytc1*) or cytochrome c oxidase, subunit IV, isoform 2 (*Cox4.2*), both components of Complex III. However, while in control adipocytes hypoxia induced a 32% and 66% decrease in *Cytc1* and *Cox4.2* expression respectively, there was no change in *Cytc1* expression, and the repression of *Cox4.2* was reduced to 44% in sh*Hif1β* cells (Figure 6d). Likewise, in control adipocytes, treatment with $CoCl_2$ produced a 20% decrease in *Cytc1* expression and a 44% decrease in *Cox4.2* expression, and these reductions were lost in the sh*Hif1β* adipocytes (Figure 6d). Thus, *Hif1β* is critical for the transition into the hypoxic state, and this involves repression of components of mitochondrial Complex III.

The roles of *Hif1β* in adipocytes are partially mediated by Hif1α

The data above show that ablation of *Hif1β* in adipocytes *in vivo* and *in vitro* leads to changes in the expression of glucose transporters, *Vegf*, and components of the mitochondrial electron transport chain. Since *Hif1β* acts as an obligate heterodimeric partner

for all *Hif-α* isoforms, as well as *Ahr*, we created stable knockdown 3T3-L1 cell lines for the two dominant forms of *Hif-α* (1 and 2) and *Ahr* to elucidate which of these factors might be acting with *Hif1β* to regulate these effects. qPCR analysis of differentiated sh*Hif1α*, sh*Hif2α*, sh*Ahr*, and shSCR (control) adipocytes, demonstrated specific knockdowns of each transcription factor by 75-88% (Figure S6a), although knockdown of *Hif1α* did lead to a 3.5-fold compensatory increase in *Hif2α* levels. Western blot analysis of cell lines under hypoxic conditions confirmed ablation of *Hif1α* and *Ahr* in sh*Hif1α* and sh*Ahr* cell lines, respectively (Figure S6b).

shSCR, sh*Hif1α*, sh*Hif2α*, and sh*Ahr* 3T3-L1 adipocytes differentiated using a standard induction protocol including 10 nM rosiglitizone displayed no difference in lipid accumulation as visualized by Oil Red O staining (Figure 7a) or quantitation of cellular triglycerides (Figure S6d). However, there was a 50% reduction in *Cebpα*, *Cebpβ*, and *aP2*, but no differences in *Pparγ*, in differentiated sh*Hif1α* adipocytes. No changes in these adipocyte differentiation markers were found in differentiated sh*Hif2α* adipocytes, and sh*Ahr* cell lines had a significant ~2-fold increase in *Cebpα* and *aP2* compared to controls (Figure S6c).

sh*Hif1α* adipocytes also had a defect in glucose uptake, with a 76% decrease in basal glucose uptake and a 55% to 88% decrease in insulin-stimulated glucose uptake (Figure 7b) that as similar to the decrease following *Hif1β* ablation (Figures 3b, 4d). By contrast, insulin-stimulated glucose uptake was unchanged in the sh*Ahr* adipocytes and was increased 3-fold in sh*Hif2α* adipocytes (Figure 7b). Interestingly, neither G*lut4* nor *Vegf* expression levels were significantly changed in any of the knockdown cell lines (Figure 7c). As with sh*Hif1α* cells, *Glut1* expression in the sh*Hif1α* cell line was decreased by 67% to 75% in all conditions. Likewise, the repression of *Cytc1* during hypoxia and $CoCl_2$ treatment that was lost upon *Hif1β* knockdown was also absent upon knockdown of *Hif1α*, but was normal in *Hif2α* or *Ahr* cells (Figure 7c). On the other hand,,*Cox4.2* expression was efficiently repressed by both hypoxia and $CoCl_2$ treatment in all knockdown cell lines. These data demonstrate that signaling through *Hif1α* is critical for some, but not all, processes controlled by *Hif1β* in adipocytes.

Discussion

In obesity, adipose tissue expands cells further from vessels become hypoxic, and this contributes to adipose tissue dysfunction (Trayhurn et al., 2008). Hypoxia in adipocytes has been demonstrated in several rodent models of obesity (Rausch et al., 2008; Ye et al., 2007; Hosogai et al., 2007), and is also present in humans, as shown by multiple lines of evidence. First, obesity leads to hypoperfusion of adipose tissue (Stuart, I et al., 2009). Secondly, *Hif-1α* expression is increased in the adipose tissue of obese individuals, and this can be reversed by weight loss (Cancello et al., 2005). Finally, all Hif-α subunits have been shown to have roles in adipocyte differentiation and function (Halberg et al., 2009; Regazzetti et al., 2009; Shimba et al., 2004; Hatanaka et al., 2009).Understanding the roles of individual Hif proteins, however, is complicated by the ability of different Hif-α subunits to at least partially compensate for one another, as illustrated by the partially overlapping target gene sets of *Hif1α* and *Hif2α* (Hu et al., 2003). Therefore, in the present study, to explore the role of the integrated Hif signaling system in adipose tissue we utilized a fat-specific ablation of the obligate heterodimeric partner for all Hif-α subunits, *Hif1β*.

We find that both male and female mice lacking *Hif1β* in fat (FH1βKO mice) are protected against age and diet-induced obesity. Indirect calorimetry revealed that this is associated with increased energy expenditure. FH1βKO mice also exhibit striking protection against obesity-related glucose intolerance and insulin resistance. Interestingly, despite the fact they

are leaner, the inflammatory and fibrotic response in fat after HFD is unchanged in FH1βKO mice. Thus, deletion of *Hif1β* in adipocytes protects against some, but not all, of the changes induced by HFD.

Ablation of *Hif1β* in fat protects against obesity by causing reduced adipocyte cell size. The primary sources of triglyceride synthesis, which determines adipocyte cell size, are *de novo* lipogenesis and fatty acid uptake from plasma. Based on cellular models, uptake of radiolabeled C^{14} palmitate is unchanged by loss of *Hif1β* Thus, the primary defect leading to a reduction in adipose tissue size following *Hif1β* ablation is a defect in *de novo* lipogenesis. Both *in vivo* and *in vitro*, loss of *Hif1β* causes a reduction in the expression of the *Glut1* and *Glut4* glucose transporters. *Glut1* is a well-known target of the hypoxia response and has been shown to be dependent on signaling by the *Hif1a/Hif1β* complex (Hayashi et al., 2004). In 3T3-L1cells, *Hif 2a* can also regulate *Glut1* and *Glut4* (Shimba et al., 2004). In FH1KO adipocytes and *Hif1β* knockdown 3T3-L1 adipocytes, this reduction in glucose transporters leads to decreased glucose uptake and a reduction of *de novo* lipogenesis, resulting in decreased adipocytes cell size.

It is likely that the ~50% reduction of glucose transporters observed when *Hif1β* is ablated plays an important role in the reduced glucose uptake and the smaller adipocytes in the FH1βKO mice. Ablation of *Glut4 alone* in adipose tissue results in a marked decrease in insulin stimulated glucose uptake, leading to glucose intolerance and insulin resistance, but without change in adipose cell size (Abel et al., 2001). By contrast, whole body haploinsuffiency of *Glut1* leads to defects in development (Wang et al., 2006) and an altered cellular response to hypoxic stress (Heilig et al., 2003). Stable knockdown of *Glut4* in 3T3-L1 adipocytes leads to decreased lipid accumulation, and the knockdown of *Glut1* and *Glut4* in combination leads to an almost complete absence of basal and insulin mediated glucose uptake (Liao et al., 2006).

In addition to the reduced glucose uptake, there is a significant down regulation in expression of key lipogenic enzymes in FH1βKO fat during HFD exposure. To what extent this is cause or effect of reduced adipose mass is difficult to assess, since previous studies have demonstrated that smaller adipocytes have lower levels of lipogenic gene expression (Bluher et al., 2004). Therefore, it is likely that *Hif1β* ablation causes a primary defect in glucose uptake which, in turn, leads to reduced adipocyte cell size and reduced lipogenic gene expression, since in 6-week FH1βKO mice, there is no decrease in fat mass and lipogenic gene expression in adipose tissue is normal.

In general, the transcription of *Hif-1* target genes serves to alter cellular responses and the local microenvironment to alleviate the hypoxia stress. A key component of this response is to promote angiogenesis through increased expression of the *Hif-1* target gene *Vegf* (Forsythe et al., 1996). Ablation of *Hif1β* both *in vivo* and *in vitro* leads to a significant decrease of *Vegf* mRNA and protein. This reduction in *Vegf* does not lead to a reduction of vessel or capillary density in the fat in either chow or HFD-challenged animals FH1βKO mice. However, prior to any change in body or fat mass, the reduction in *Vegf* leads to a significantly decreased vascular permeability, as assessed by Evans Blue extravasation of dye.. Additionally, increased vascular permeability, has been shown to be central to the adipose tissue expansion induced by thiazolidinediones treatment (Sotiropoulos et al, 2006). On the other hand, previous studies have shown that increases in adipocyte mass can be altered by angiogenesis inhibitors (Rupnick et al., 2002). Likewise, blocking Vegf action by treating mice with antibodies to the Vegf receptor has been shown to reduce weight gain during diet induced obesity (Tam et al., 2009). Thus, the changes we observe in *Vegf* and vascular permeability could contribute to the reduction of adipocyte hypertrophy in the FH1βKO animals.

There is a well-established link between mitochondrial activity and hypoxia. Previous studies have demonstrated that reactive oxygen species produced by the mitochondria (mtROS) are essential for oxygen sensing and *Hif1α/Hif2α* stabilization during hypoxia. In particular, mtROS generated from Complex III has been shown to be necessary for regulating *Hif1α* and *Hif2α* (Guzy et al., 2005; Bell et al., 2007), and loss of the Complex III protein, cytochrome c impairs cellular oxygen sensing and *Hif1α* activation in response to hypoxia (Mansfield et al., 2005). In this study, we find that *Hif1β* is necessary for the down-regulation of *Cytc1* which occurs during hypoxia and after treatment with the hypoxia mimetic $CoCl_2$. Interestingly, adipose tissue from mice with fat specific knockout of the insulin receptor (FIRKO mice) exhibits lower levels of *Hif1α* and higher levels of *Cytc1* (Katic et al., 2007). It is likely that the smaller adipocytes present in the FIRKO mice have lower levels of hypoxia, and thus retain higher levels of mitochondrial activity. The results presented here further elucidate that relationship by demonstrating the coordination of these hypoxia and mitochondrial activity in an entirely different model system.

In the lung and liver, *Hif1α* has been shown to regulate *Cox4.1* and *Cox4.2* expression (Fukuda et al., 2007). Reduced oxygen availability leads to an increase in transcription of *Cox4.2* and *Lon*, the mitochondrial protease required for *Cox4.1* degradation and optimization of respiratory efficiency. In contrast to these findings, in adipocytes from normal mice there is a decrease in expression of *Cox4.2* after exposure to hypoxia or treatment with $CoCl_2$ treatment and no change in C*ox4.1* expression, while expression of *Lon* is increased by hypoxia, but not $CoCl_2$. In adipocytes, this repression of C*ox4.2*, but not the increased expression of *Lon*, is dependent on the presence of *Hif1β* (Figure S7c,d). Thus, the regulation of *Cox4.1* and *Cox4.2* expression in response to hypoxia is different in adipocytes than in the liver or lung.

The relationship of these changes in gene expression to other markers of hypoxic stress is complex. Immunohistochemical staining for pimonidazole adducts, which mark hypoxic areas, show that hypoxia within the fat pads of young control and FH1βKO animals is relatively low. However, in HFD-induced obesity, hypoxic regions can be found scattered through both the subcutaneous and perigonadal fat pads of control mice, and also found in FH1βKO mice despite their protection from adipocytes hypertrophy and obesity. Levels of the pro-inflammatory cytokines *Tnfα* and *Mcp1* and macrophage infiltration are increased by HFD in control mice as expected, and again this was unchanged in FH1βKO mice despite the smaller adipocytes and fat pad weight. Additionally, consistent with previous studies in the *ob/ob* mouse (Halberg et al., 2009), we observed increased expression of numerous markers of fibrosis including *mLox*, *Col6a1*, and *Col1a1*, after 12 weeks of HFD, and these markers were unchanged by *Hif1β* ablation. Thus, despite protection from adipocytes enlargement and obesity, FH1βKO mice still exhibit evidence of increased fibrosis and inflammation in response to HFD.

FH1βKO mice display normal brown fat morphology on normal and HFD, but show increased capillary density compared to controls after HFD exposure. This is in contrast to effects of adipose specific expression of a dominant negative *Hif1α* which results decreases in mitochondrial content and vascular density in the BAT leading to obesity, glucose intolerance, and insulin resistance (Zhang et al., 2010). An important difference between these two models is that ablation of *Hif1β* not only inhibits *Hif1α* signaling, but also inhibits the actions of *Hif2α* and *Ahr*. This is in keeping with our findings that in cultured cells, we find that *Hif1α* and *Hif2α* have distinct roles in adipocyte biology. Ablation of *Hif1α* reduces glucose uptake, whereas ablation of *Hif2α* enhances glucose uptake. Interestingly, *Hif2α* is upregulated in *Hif1α* knockout cells. These data suggest an important role for *Hif2α* in adipocytes. *Hif1β* may also exert effects by partnering with the aryl hydrocarbon receptor *Ahr*. Knockdown of *Ahr* in 3T3-L1 adipocytes leads to an increase in the differentiation

markers *Cebpα* and *aP2*, supporting previous experiments that demonstrate *Ahr* is a negative regulator of adipogenesis that affects expression of *Cebpα*, and subsequently, *aP2* (Alexander et al., 1998; Shimba et al., 2001). Thus, attenuation of *Ahr* activity by ablation of *Hif1β* in the adipose tissue of FH1βKO may lead to an enhanced differentiation capacity that rescues differentiation defect observed in the BAT of dominant negative *Hif1α* mice.

Both sh*Hif1β* and sh*Hif1α* adipocytes exhibit reduced expression of *Glut1*, reduced glucose uptake and a lack of repression of *Cytc1* in response to hypoxia. However, other changes molecular changes, including reduced *Glut4* and *Vegf* expression, as well as, the loss of *Cox4.2* repression observed in the sh*Hif1β* adipocytes are not observed after ablation of the interacting partners. These data suggest that *Hif1β* alters signaling through other pathways or that there is redundancy between these interacting partners.

In conclusion, *Hif1β* (*Arnt*) plays a pivotal role in adipose tissue by controlling glucose uptake, expression of *Vegf*, and regulation of the hypoxia in a cell autonomous manner response. The altered *Vegf* expression results in secondary cell, or non-autonomous, changes in vascular permeability. Together, these effects control adipose growth and triglyceride accumulation. Thus, reducing *Hif1β* in adipose tissue limits the effects of hypoxia on adipose tissue in the obese state and may represent a novel therapeutic target for treatment of obesity.

Supplementary Material

Refer to Web version on PubMed Central for supplementary material.

Acknowledgments

The authors would like to thank Dr. Frank J. Gonzalez (National Cancer Institute) for the *Hif1β* floxed mice. We are grateful to M. Rourk and G. Smyth for animal care; C. Cahill (Joslin DERC Advanced Microscopy Core); and A. Clermont, M. Poillucci (DERC Physiology Core), H. Li (DERC Specialized Assay Core), and J. Schroeder (DERC Genomics Core) for technical assistance. This work was supported by the Joslin Training Grant (T32DK007260), NIH grants DK 60837 and DK 82655, an American Diabetes Association mentor-based award, and the Mary K. Iacocca Professorship to C.R. Kahn.

APPENDIX

Material and Methods

Further details on many of the experimental methods including the maintenance of mice, metabolic analysis, glucose and palmitate uptake, lipogensis, lipolysis, cell culture, cloning, histology, antibodies utilized, and the oxygen consumption assays can be found in the Supplemental Experimental Procedures.

Animals and diets

aP2-cre and *Hif1β* floxed animals have previously been described (Abel et al., 2001; Tomita et al., 2000). Animal care and study protocols were approved by the Animal Care Committee of Joslin Diabetes Center.

Body composition and metabolic analysis

Body composition was measured using a Lunar PIXImus2 densitometer (GE Medical Systems). Adipocyte diameters from FH1βKO and control mice at 6-8 weeks old, 20 weeks old, and after 12 weeks of HFD exposure were calculated using Image J software Activity was measured using the OPTO-M3 sensor system (Comprehensive Laboratory Animal Monitoring System, CLAMS; Columbus Instruments). Indirect calorimetry was measured

on the same mice using an open-circuit Oxymax system (Columbus Instruments). Intraperitoneal glucose (2 g/kg weight) and insulin tolerance (1.25 unit/kg) tests were performed after a 16- and 4-h fast, respectively. Insulin, free fatty acids, leptin, adiponectin were measured by ELISA (Crystal Chem). Adipocyte diameters were calculated using Image J software.

Analysis of gene expression

Total RNA was isolated using an RNeasy minikit (Qiagen), and cDNA was synthesized with the High Capacity cDNA Reverse Transcription Kit (Applied Biosystems). Gene expression was determined by RT-qPCR performed on a ABI Prism 7900HT sequence.

Lentiviral infection and 3T3-L1 differentation

Hif1β, *Hif1α*, *Hif2α*, and *Ahr* were stably knocked-down in 3T3-L1 cells by shRNA delivered by lentiviral infection and selected with puromycin. Differentiation was induced by exposing the cells 1 μM dexamethasone, 500 μM isobutylmethylxanthine and 100 nM insulin for two days. Except for the assessment of differentiation capacity, the PPARγ agonist 1 μM rosiglitazone was added in all experiments. Cells were then grown for six days in 100 nM insulin. Medium was replaced every other day.

Histology

Vascularity in the fat pads was determined by whole mount *CD31* immunofluorescence and staining of GSL I – isolectin B4. For permeability analysis, Evans blue dye was administered by intra-cardiac injection followed by perfusion with phosphate buffered saline. Lipids from liver samples and differentiated culture plates were visualized and quantified by Oil Red O staining.

Oxygen consumption assay

Oxygen consumption was measured using the XF24 Extracellular Flux Analyzer from Seahorse Bioscience. A bioenergetics profile was determined by sequential injections of oligomycin, FCCP, and rotenone.

Statistics

All differences were analyzed by Student’s t-test. Results were considered significant if $p<0.05$.

References

Abel ED, Peroni O, Kim JK, Kim YB, Boss O, Hadro E, Minnemann T, Shulman GI, Kahn BB. Adipose-selective targeting of the GLUT4 gene impairs insulin action in muscle and liver. Nature. 2001; 409:729–733. [PubMed: 11217863]

Alexander DL, Ganem LG, Fernandez-Salguero P, Gonzalez F, Jefcoate CR. Aryl-hydrocarbon receptor is an inhibitory regulator of lipid synthesis and of commitment to adipogenesis. J Cell Sci. 1998; 111(Pt 22):3311–3322. [PubMed: 9788873]

Bray GA. Medical consequences of obesity. J Clin Endocrinol Metab. 2004; 89:2583–9. [PubMed: 15181027]

Bell EL, Klimova TA, Eisenbart J, Moraes CT, Murphy MP, Budinger GR, Chandel NS. The Qo site of the mitochondrial complex III is required for the transduction of hypoxic signaling via reactive oxygen species production. J Cell Biol. 2007; 177:1029–1036. [PubMed: 17562787]

Bluher M, Patti ME, Gesta S, Kahn BB, Kahn CR. Intrinsic heterogeneity in adipose tissue of fat-specific insulin receptor knock-out mice is associated with differences in patterns of gene expression. J Biol Chem. 2004; 279:31891–31901. [PubMed: 15131119]

Cancello R, Henegar C, Viguerie N, Taleb S, Poitou C, Rouault C, Coupaye M, Pelloux V, Hugol D, Bouillot JL, Bouloumie A, Barbatelli G, Cinti S, Svensson PA, Barsh GS, Zucker JD, Basdevant A, Langin D, Clement K. Reduction of macrophage infiltration and chemoattractant gene expression changes in white adipose tissue of morbidly obese subjects after surgery-induced weight loss. Diabetes. 2005; 54:2277–2286. [PubMed: 16046292]

Chen D, Elmendorf JS, Olson AL, Li X, Earp HS, Pessin JE. Osmotic shock stimulates GLUT4 translocation in 3T3L1 adipocytes by a novel tyrosine kinase pathway. J Biol Chem. 1997; 272:27401–27410. [PubMed: 9341192]

Compernolle V, Brusselmans K, Acker T, Hoet P, Tjwa M, Beck H, Plaisance S, Dor Y, Keshet E, Lupu F, Nemery B, Dewerchin M, Van Veldhoven P, Plate K, Moons L, Collen D, Carmeliet P. Loss of HIF-2 and inhibition of VEGF impair fetal lung maturation, whereas treatment with VEGF prevents fatal respiratory distress in premature mice. Nat Med. 2002; 7:702–10. [PubMed: 12053176]

Forsythe JA, Jiang BH, Iyer NV, Agani F, Leung SW, Koos RD, Semenza GL. Activation of vascular endothelial growth factor gene transcription by hypoxia-inducible factor 1. Mol Cell Biol. 1996; 16:4604–4613. [PubMed: 8756616]

Fukuda R, Zhang H, Kim JW, Shimoda L, Dang CV, Semenza GL. HIF-1 regulates cytochrome oxidase subunits to optimize efficiency of respiration in hypoxic cells. Cell. 2007; 129:111–122. [PubMed: 17418790]

Guzy RD, Hoyos B, Robin E, Chen H, Liu L, Mansfield KD, Simon MC, Hammerling U, Schumacker PT. Mitochondrial complex III is required for hypoxia-induced ROS production and cellular oxygen sensing. Cell Metab. 2005; 1:401–408. [PubMed: 16054089]

Gunton JE, Kulkarni RN, Yim S, Okada T, Hawthorne WJ, Tseng YH, Roberson RS, Ricordi C, O'Connell PJ, Gonzalez FJ, Kahn CR. Loss of ARNT/HIF1beta mediates altered gene expression and pancreatic-islet dysfunction in human type 2 diabetes. Cell. 2005; 3:337–49. 2005. [PubMed: 16096055]

Halberg N, Khan T, Trujillo ME, Wernstedt-Asterholm I, Attie AD, Sherwani S, Wang ZV, Landskroner-Eiger S, Dineen S, Magalang UJ, Brekken RA, Scherer PE. Hypoxia-inducible factor 1alpha induces fibrosis and insulin resistance in white adipose tissue. Mol Cell Biol. 2009; 29:4467–4483. [PubMed: 19546236]

Hatanaka M, Shimba S, Sakaue M, Kondo Y, Kagechika H, Kokame K, Miyata T, Hara S. Hypoxia-inducible factor-3alpha functions as an accelerator of 3T3-L1 adipose differentiation. Biol Pharm. Bull. 2009; 32:1166–1172. [PubMed: 19571379]

Hayashi M, Sakata M, Takeda T, Yamamoto T, Okamoto Y, Sawada K, Kimura A, Minekawa R, Tahara M, Tasaka K, Murata Y. Induction of glucose transporter 1 expression through hypoxia-inducible factor 1alpha under hypoxic conditions in trophoblast-derived cells. J Endocrinol. 2004; 183:145–154. [PubMed: 15525582]

Heilig C, Brosius F, Siu B, Concepcion L, Mortensen R, Heilig K, Zhu M, Weldon R, Wu G, Conner D. Implications of glucose transporter protein type 1 (GLUT1)-haplodeficiency in embryonic stem cells for their survival in response to hypoxic stress. Am J Pathol. 2003; 163:1873–1885. [PubMed: 14578187]

Hosogai N, Fukuhara A, Oshima K, Miyata Y, Tanaka S, Segawa K, Furukawa S, Tochino Y, Komuro R, Matsuda M, Shimomura I. Adipose tissue hypoxia in obesity and its impact on adipocytokine dysregulation. Diabetes. 2007; 56:901–911. [PubMed: 17395738]

Hu CJ, Wang LY, Chodosh LA, Keith B, Simon MC. Differential roles of hypoxia-inducible factor 1alpha (HIF-1alpha) and HIF-2alpha in hypoxic gene regulation. Mol Cell Biol. 2003; 23:9361–9374. [PubMed: 14645546]

Iyer NV, Kotch LE, Agani F, Leung SW, Laughner E, Wenger RH, Gassmann M, Gearhart JD, Lawler AM, Yu AY, Semenza GL. Cellular and developmental control of O2 homeostasis by hypoxia-inducible factor 1 alpha. Genes. Dev. 1998; 12:149–162. [PubMed: 9436976]

Kaluz S, Kaluzova M, Stanbridge EJ. Regulation of gene expression by hypoxia: integration of the HIF-transduced hypoxic signal at the hypoxia-responsive element. Clin Chim. Acta. 2008; 395:6–13. [PubMed: 18505681]

Katic M, Kennedy AR, Leykin I, Norris A, McGettrick A, Gesta S, Russell SJ, Bluher M, Maratos-Flier E, Kahn CR. Mitochondrial gene expression and increased oxidative metabolism: role in

increased lifespan of fat-specific insulin receptor knock-out mice. Aging. Cell. 2007; 6:827–839. [PubMed: 18001293]

Keith B, Adelman DM, Simon MC. Targeted mutation of the murine arylhydrocarbon receptor nuclear translocator 2 (Arnt2) gene reveals partial redundancy with Arnt. Proc Natl. Acad Sci U S. A. 2001; 98:6692–6697. [PubMed: 11381139]

Liao W, Nguyen MT, Imamura T, Singer O, Verma IM, Olefsky JM. Lentiviral short hairpin ribonucleic acid-mediated knockdown of GLUT4 in 3T3-L1 adipocytes. Endocrinology. 2006; 147:2245–52. [PubMed: 16497797]

Maltepe E, Schmidt JV, Baunoch D, Bradfield CA, Simon MC. Abnormal angiogenesis and responses to glucose and oxygen deprivation in mice lacking the protein ARNT. Nature. 1997; 386:403–407. [PubMed: 9121557]

Mansfield KD, Guzy RD, Pan Y, Young RM, Cash TP, Schumacker PT, Simon MC. Mitochondrial dysfunction resulting from loss of cytochrome c impairs cellular oxygen sensing and hypoxic HIF-alpha activation. Cell Metab. 2005; 1:393–399. [PubMed: 16054088]

Peng J, Zhang L, Drysdale L, Fong GH. The transcription factor EPAS-1/hypoxia-inducible factor 2alpha plays an important role in vascular remodeling. Proc Natl. Acad Sci U S. A. 2000; 97:8386–8391. [PubMed: 10880563]

Rankin EB, Higgins DF, Walisser JA, Johnson RS, Bradfield CA, Haase VH. Inactivation of the arylhydrocarbon receptor nuclear translocator (Arnt) suppresses von Hippel-Lindau disease-associated vascular tumors in mice. Mol Cell Biol. 2005; 25:3163–3172. [PubMed: 15798202]

Rausch ME, Weisberg S, Vardhana P, Tortoriello DV. Obesity in C57BL/6J mice is characterized by adipose tissue hypoxia and cytotoxic T-cell infiltration. Int. J Obes. (Lond.). 2008; 32:451–463. [PubMed: 17895881]

Regazzetti C, Peraldi P, Gremeaux T, Najem-Lendom R, Ben Sahra I, Cormont M, Bost F, Marchand-Brustel Y, Tanti JF, Giorgetti-Peraldi S. Hypoxia decreases insulin signaling pathways in adipocytes. Diabetes. 2009; 58:95–103. [PubMed: 18984735]

Rupnick MA, Panigrahy D, Zhang CY, Dallabrida SM, Lowell BB, Langer R, Folkman MJ. Adipose tissue mass can be regulated through the vasculature. Proc Natl. Acad Sci U S. A. 2002; 99:10730–10735. [PubMed: 12149466]

Scortegagna M, Ding K, Oktay Y, Gaur A, Thurmond F, Yan LJ, Marck BT, Matsumoto AM, Shelton JM, Richardson JA, Bennett MJ, Garcia JA. Multiple organ pathology, metabolic abnormalities and impaired homeostasis of reactive oxygen species in Epas1−/− mice. Nat Genet. 2003; 4:331–40. [PubMed: 14608355]

Sekine H, Mimura J, Yamamoto M, Fujii-Kuriyama Y. Unique and overlapping transcriptional roles of arylhydrocarbon receptor nuclear translocator (Arnt) and Arnt2 in xenobiotic and hypoxic responses. J Biol Chem. 2006; 281:37507–37516. [PubMed: 17023418]

Shimba S, Wada T, Hara S, Tezuka M. EPAS1 promotes adipose differentiation in 3T3-L1 cells. J Biol Chem. 2004; 279:40946–40953. [PubMed: 15258146]

Shimba S, Wada T, Tezuka M. Arylhydrocarbon receptor (AhR) is involved in negative regulation of adipose differentiation in 3T3-L1 cells: AhR inhibits adipose differentiation independently of dioxin. J Cell Sci. 2001; 114:2809–2817. [PubMed: 11683414]

Sotiropoulos KB, Clermont A, Yasuda Y, Rask-Madsen C, Mastumoto M, Takahashi J, Della Vecchia K, Kondo T, Aiello LP, King GL. Adipose-specific effect of rosiglitazone on vascular permeability and protein kinase C activation: novel mechanism for PPARgamma agonist's effects on edema and weight gain. FASEB J. 2006; 8:1203–5. [PubMed: 16672634]

Stuart W,I, de Heredia FP, Wang B, Trayhurn P. Cellular hypoxia and adipose tissue dysfunction in obesity. Proc Nutr Soc. 2009; 68:370–377. [PubMed: 19698203]

Swanson HI, Chan WK, Bradfield CA. DNA binding specificities and pairing rules of the Ah receptor, ARNT, and SIM proteins. J Biol Chem. 1995; 270:26292–26302. [PubMed: 7592839]

Tam J, Duda DG, Perentes JY, Quadri RS, Fukumura D, Jain RK. Blockade of VEGFR2 and not VEGFR1 can limit diet-induced fat tissue expansion: role of local versus bone marrow-derived endothelial cells. PLoS. One. 2009; 4:e4974. [PubMed: 19333381]

Tian H, Hammer RE, Matsumoto AM, Russell DW, McKnight SL. The hypoxia-responsive transcription factor EPAS1 is essential for catecholamine homeostasis and protection against heart failure during embryonic development. Genes. Dev. 1998; 12:3320–3324. [PubMed: 9808618]

Tomita S, Sinal CJ, Yim SH, Gonzalez FJ. Conditional disruption of the aryl hydrocarbon receptor nuclear translocator (Arnt) gene leads to loss of target gene induction by the aryl hydrocarbon receptor and hypoxia-inducible factor 1alpha. Mol Endocrinol. 2000; 14:1674–1681. [PubMed: 11043581]

Trayhurn P, Wang B, Wood IS. Hypoxia and the endocrine and signalling role of white adipose tissue. Arch. Physiol. Biochem. 2008; 114:267–276. [PubMed: 18946787]

Trayhurn P, Wood IS. Adipokines: inflammation and the pleiotropic role of white adipose tissue. Br. J Nutr. 2004; 92:347–355. [PubMed: 15469638]

Wang D, Pascual JM, Yang H, Engelstad K, Mao X, Cheng J, Yoo J, Noebels JL, De Vivo DC. A mouse model for Glut-1 haploinsufficiency. Hum. Mol Genet. 2006; 15:1169–1179. [PubMed: 16497725]

Wang XL, Suzuki R, Lee K, Tran T, Gunton JE, Saha AK, Patti ME, Goldfine A, Ruderman NB, Gonzalez FJ, Kahn CR. Ablation of ARNT/HIF1beta in liver alters gluconeogenesis, lipogenic gene expression, and serum ketones. Cell Metab. 2009; 5:428–39. [PubMed: 19416713]

Yamauchi T, Kamon J, Waki H, Terauchi Y, Kubota N, Hara K, Mori Y, Ide T, Murakami K, Tsuboyama-Kasaoka N, Ezaki O, Akanuma Y, Gavrilova O, Vinson C, Reitman ML, Kagechika H, Shudo K, Yoda M, Nakano Y, Tobe K, Nagai R, Kimura S, Tomita M, Froguel P, Kadowaki T. The fat-derived hormone adiponectin reverses insulin resistance associated with both lipoatrophy and obesity. Nat. Med. 2001; 7:941–946. [PubMed: 11479627]

Ye J, Gao Z, Yin J, He Q. Hypoxia is a potential risk factor for chronic inflammation and adiponectin reduction in adipose tissue of ob/ob and dietary obese mice. Am J Physiol. Endocrinol Metab. 2007; 293:E1118–E1128. [PubMed: 17666485]

Zhang X, Lam KS, Ye H, Chung SK, Zhou M, Wang Y, Xu A. Adipose tissue-specific inhibition of hypoxia-inducible factor 1{alpha} induces obesity and glucose intolerance by impeding energy expenditure in mice. J Biol Chem. 2010; 285:32869–32877. [PubMed: 20716529]

Highlights

- ice lacking Hif1β in fat are protected from obesity and glucose intolerance.
- Mice lacking Hif1β in fat have reduced VEGF and vascular permeability in fat.
- Hif1β regulates glucose uptake in fat both *in vivo* and *in vitro*.
- Hif1β regulates cellular respiration and mitochondrial genes in response to hypoxia.

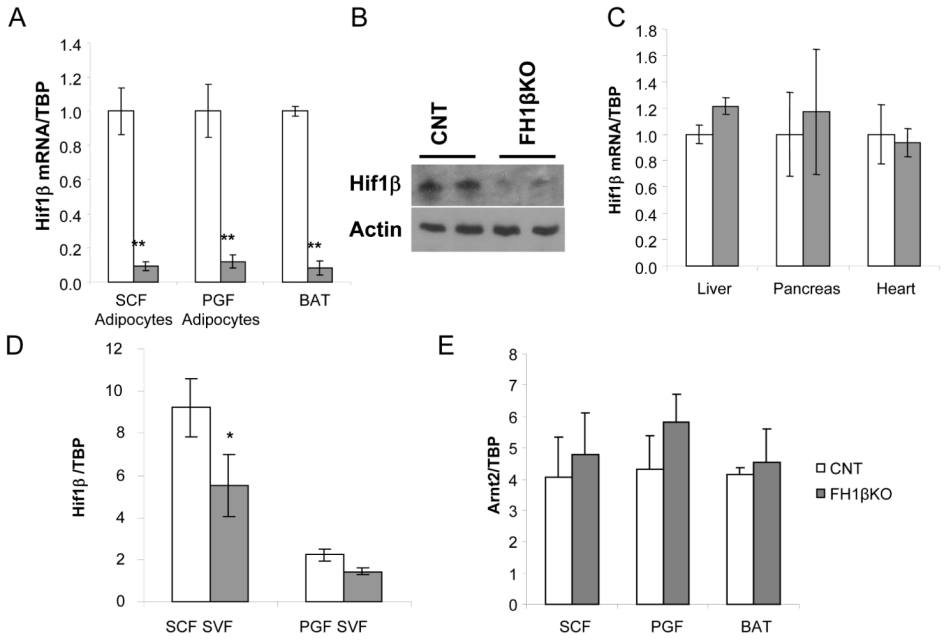

Figure 1. aP2-Cre effectively ablates *Hif1β* in adipocytes

A) Expression level of *Hif1β* mRNA was compared using quantitative real-time PCR (qPCR) between adipocytes isolated from the subcutaneous fat (SCF) and perigonadal fat (PGF) and whole brown adipose tissue (BAT) in female control and FH1βKO mice. Mice were 6-8 weeks of age. Data are shown as mean ± SEM of five samples. Asterisks indicate $p<0.05$ in all panels.

B) Western blot of *Hif1β* from isolated PGF adipocytes of control and FH1βKO mice at 12 weeks of age. Actin served as a loading control. Data are representative of four samples.

C) Expression level of *Hif1β* mRNA by qPCR in liver, pancreas and heart of female control and FH1βKO mice. Mice were 6-8 weeks old. Data are shown as mean ± SEM of four samples.

D) Expression level of *Hif1β* mRNA by qPCR of stromovascular fraction (SVF) isolated from subcutaneous or perigonadal in control and FH1βKO mice. Mice were 6-8 weeks of age. Data are shown as mean ± SEM of four samples.

E) Expression level of Arnt2 mRNA was compared using qPCR in samples from

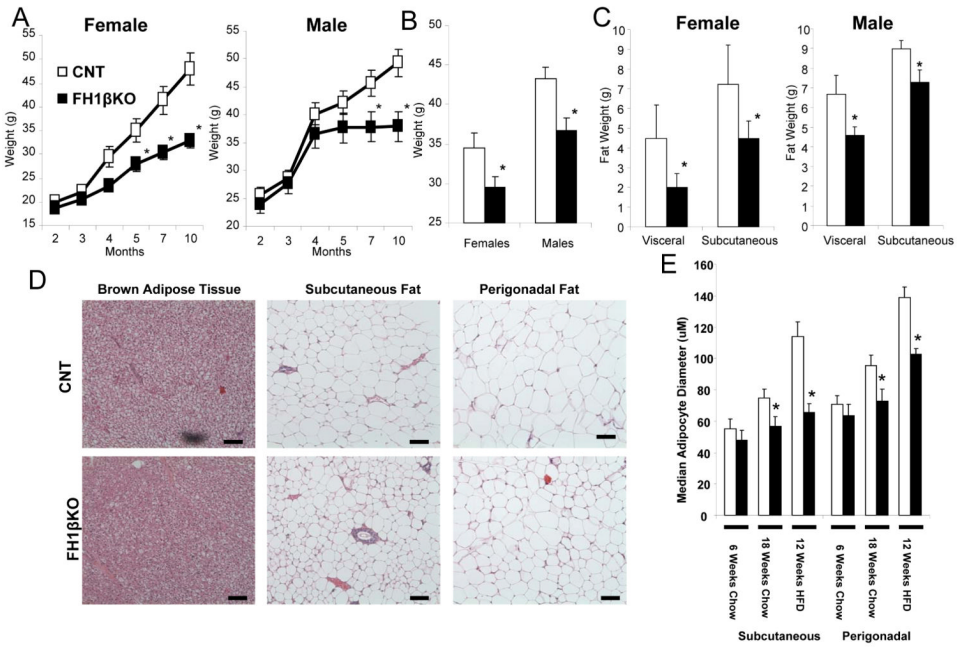

Figure 2. Ablation of *Hif1β* attenuates age and diet induced obesity

A) Body weight of female and male control and FH1βKO mice on chow diet. Data are shown as mean ± SEM of 5-6 animals/group. Asterisks indicate a significant difference ($p<0.05$) in all panels.

B) Body weight of female and male control and FH1βKO after 10 weeks of high fat diet (HFD) starting at 6 weeks of age. Data are shown as mean ± SEM of 8-10 animals/group.

C) Analysis of body composition by DEXA scan of control and FH1βKO at 5 months of age. Data are shown as mean ± SEM of 4-5 animals/group.

D) Hematoxylin and eosin stained representative sections of fat pads and FH1βKO mice at 20 weeks of age on chow diet. Pictures were taken at *20x*.

E) Median adipocyte size in adipocytes. Perigonadal and subcutaneous fat from 8 wk chow fed, 20 week chow fed, and 12 weeks of HFD (started at 6 weeks) mice (n = 4/group) were hematoxylin and eosin stained with five digital images (20x) from non-overlapping fields were taken from each slide (total 20 fields per group), and adipocyte diameters were calculated using Image J software. Values are median ± SEM of 4 animals.

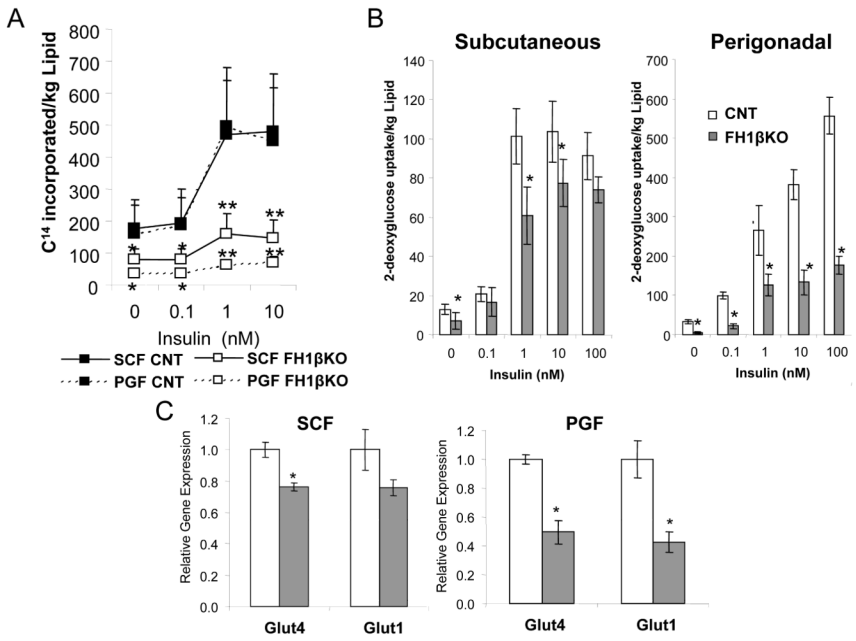

Figure 3. FH1βKO adipocytes display defects in lipogenesis, glucose uptake, and glucose transporter expression

A) [^{14}C] D-glucose incorporation into lipids in subcutaneous and perigonadal adipocytes isolated from control and FH1βKO animals at 12 weeks of age. Data are represented as ^{14}C counts and normalized to lipid content. Data shown as mean ± SEM of 4 animals/group and are representative of two independent experiments. Asterisks in all panels indicate $p<0.05$, and double asterisks indicate $p<0.01$.

B) [^{3}H] 2-deoxyglucose uptake into subcutaneous and perigonadal adipocytes isolated from control and FH1βKO animals at 15 weeks of age. Data are represented as ^{3}H counts and normalized to lipid content. Data are mean ± SEM of 4 animals/group. The entire experiment was repeated twice. Asterisks in all panels indicate $p<0.05$.

C) Expression levels of *Glut1* and *Glut4* mRNA were compared using qPCR between subcutaneous and perigonadal in male control and FH1βKO mice. Mice were 6-8 weeks old. Data are mean ± SEM of four samples.

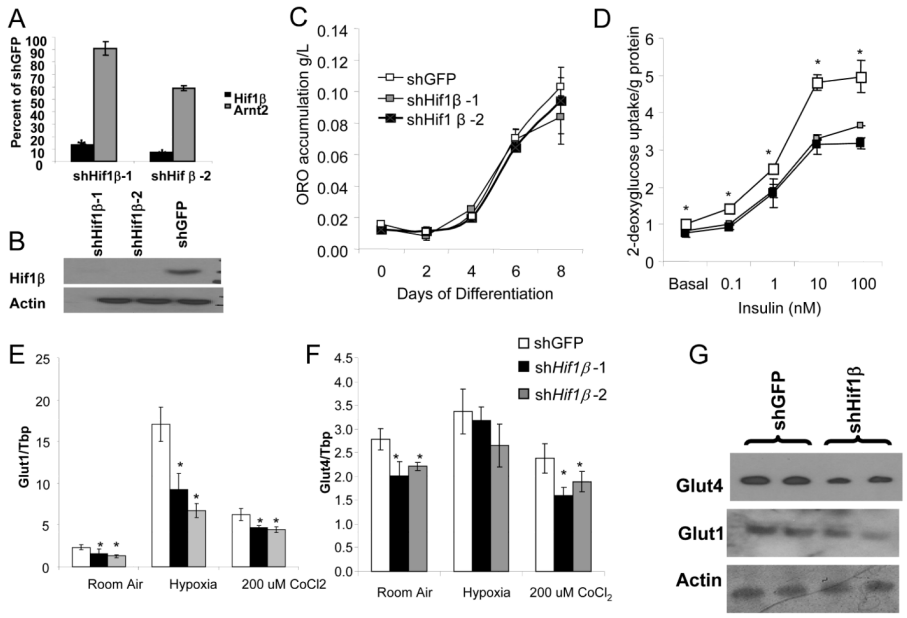

Figure 4. shRNA knockdown of *Hif1β* decreases glucose uptake

A) Expression level of *Hif1β* and *Arnt2* mRNA was compared using qPCR between 3T3-L1 preadipocytes stably transfected with sh*Hif1β*-1 and sh*Hif1β*-2. Data are normalized by relative expression of *Hif1β* and *Arnt2* mRNA in shGFP cells and are shown as mean ± SEM of triplicate samples, repeated five times. Asterisks indicate $p<0.05$ in all panels.

B) Western blot of *Hif1β* from protein extracts from 3T3-L1 preadipocytes stably transfected with sh*Hif1β*-1, sh*Hif1β*-2, and shGFP cells. Actin was used as a loading control.

C) Quantification of Oil Red-O staining in shHif1β-1, shHif1β-2, and shGFP adipocytes. Data are shown as mean ± SEM of triplicate samples repeated twice. Asterisks indicate a significant difference ($p<0.05$).

D) Glucose uptake, as assessed by acute uptake of ^{3}H-labeled 2-deoxyglucose into sh*Hif1β*-1, sh*Hif1β*-2, and shGFP stably transfected adipocytes. Data are represented as ^{3}H count normalized to protein content, and are shown as mean ± SEM of triplicate samples repeated three times.

E) Expression of *Glut1* and *Glut4* as measured by qPCR. In cells with stable Knockdown of *Hif1β*-1, *Hif1β*-2 and shGFP. After eight days of differentiation, cells were subjected to normoxia, hypoxia (0.1% O_2 for 16hrs), or 200 nM $CoCl_2$ for 16 hrs. Data shown as mean ± SEM of triplicate samples and repeated three times.

F) Western blot of Glut1 and Glut4 from protein extracts from sh*Hif1β*-2 and shGFP 3T3-L1 adipocytes after eight days of differentiation. Actin was used as a loading control.

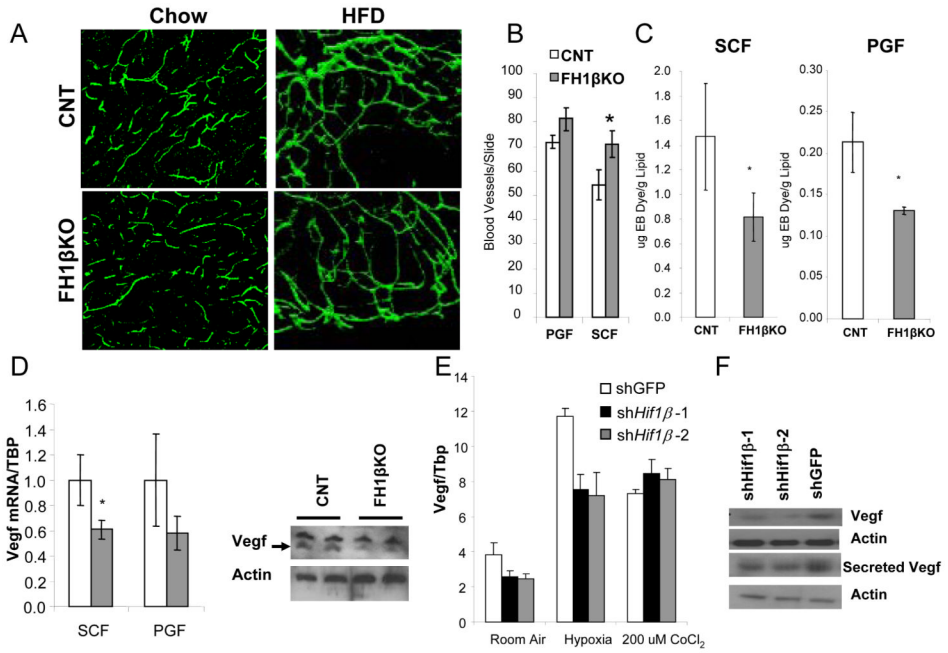

Figure 5. *Hif1β* ablation decreases vascular permeability and *Vegf* expression

A) Left panels: CD31 immunohistochemistry on whole mounts of subcutaneous fat from control and FH1βKO male mice at 8 weeks of age. The photograph was taken at 100x. Right panels: CD31 immunohistochemistry on whole mounts of subcutaneous fat from control and FH1βKO male mice after 12 weeks of exposure to high fat diet.

B) Quantitation of capillary density in the perigonadal and subcutaneous fat pads after 12 weeks on HFD, starting at 6 weeks of age (n = 4/group). Slides were stained for GSL I - isolectin B4. Capillaries were counted from three digital images (20×) from non-overlapping fields were taken from each slide (total 12 fields per group) from control and FH1βKO males. Data are shown as mean ± SEM of three samples. Asterisks indicate $p<0.05$.

C) Quantitation of the amount of Evan's blue in fat pads 10 minutes after intra-cardiac injection and perfusion into control and FH1βKO male mice at 8 weeks of age. Data are normalized by gram of lipid from fat pads and are shown as mean ± SEM of three samples. Asterisks indicate a significant difference in all panels ($p<0.05$).

D) Levels of *Vegf* mRNA were compared using qPCR between adipocytes isolated from the subcutaneous fat (SCF) and perigonadal fat (PGF). Mice were 6-8 weeks old. Data are shown as mean ± SEM of five samples. Asterisks indicate $p<0.05$. Western blot of *Vegf* from isolated PGF adipocytes of female control and FH1βKO^{-} mice at 12 weeks of age. Western blot for actin is a loading control. Data are representative of four samples.

E) mRNA was isolated from sh*Hif1β*-1, sh*Hif1β*-2, and shGFP stably transfected adipocytes after eight days of differentiation, and subjected to normoxia, hypoxia (0.1% O_2 for 16hrs), or 200 nM $CoCl_2$ for 16 hrs. Expression of *Vegf* was measured by qPCR. Data shown as mean ± SEM of triplicate samples and repeated three times.

F) Western blot of Vegf from protein extracts from 3T3-L1 adipocytes stably transfected with sh*Hif1β*-1, sh*Hif1β*-2, and shGFP adipocytes, or media secreted by sh*Hif1β*-1, sh*Hif1β*-2, and shGFP adipocytes after eight days of differentiation. Actin was used as a loading control.

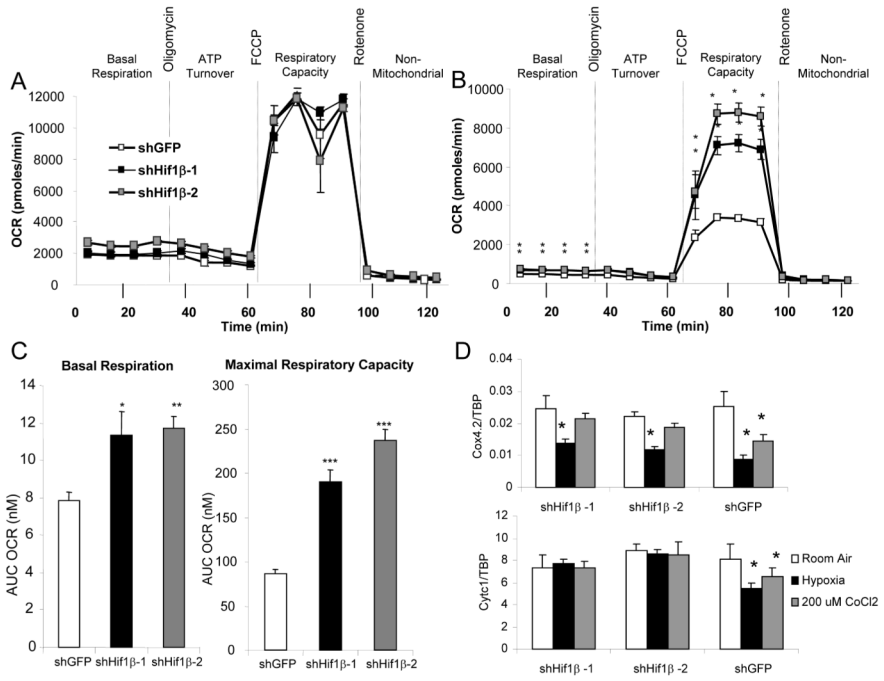

Figure 6. *Hif1 β* shRNA knockdown increases respiratory capacity during $CoCl_2$ treatment

A) Bioenergetics profile, as measured by oxygen consumption rate with a Seahorse X24 extracellular flux analyzer, of sh*Hif1β*-1, sh*Hif1β*-2, and shGFP 3T3-L1 adipocytes under normoxic conditions.

B) Bioenergetics profile, as measured by oxygen consumption rate with a Seahorse X24 extracellular flux analyzer, of sh*Hif1β*-1, sh*Hif1β*-2, and shGFP 3T3-L1 adipocytes after pre-treatment with $CoCl_2$.

C) Basal respiration and maximal respiratory capacity of sh*Hif1β*-1, sh*Hif1β*-2, and shGFP 3T3-L1 adipocytes was determined by calculating the area under the curve (AUC) in the basal phase and after uncoupling with FCCP. Values are means ± SEM of 6-7 replicates of three separate experiments. Asterisks indicate a significant difference compared to shGFP control in all panels ($p<0.05$).

D) mRNA was isolated from sh*Hif1β*-1, sh*Hif1β*-2, and shGFP stably transfected adipocytes after eight days of differentiation, and subjected to normoxia, hypoxia (0.1% O_2 for 16hrs), or 200 nM $CoCl_2$ for 16 hrs. Expression of *Cytc1* and *Cox4.2* was measured by qPCR. Data shown as mean ± SEM of triplicate samples and repeated three times.

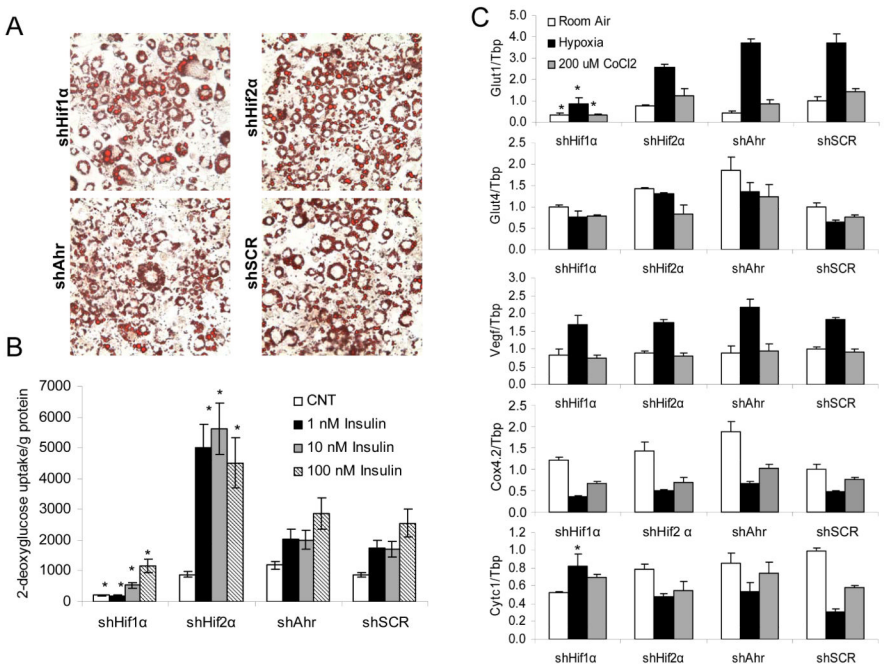

Figure 7. Ablation of *Hif1α* recapitulates a subset of the effects of *Hif1β* ablation

A) Triglyceride accumulation after 8 days of differentiation was visualized by Oil Red-O staining in sh*Hif1α*, sh*Hif2α*, sh*Ahr*, and shScr (control) adipocytes after 8 days of differentiation.

B) ^{3}H-labeled 2-deoxyglucose uptake into sh*Hif1α*, sh*Hif2α*, sh*Ahr*, and shScr stably transfected adipocytes after eight days of differentiation. Data are represented as ^{3}H counts normalized to protein content. Data shown as mean ± SEM of four samples and repeated twice. Values are means ± SEM, and asterisks indicate a significant difference compared to shSCR control with the same treatment in all panels ($p<0.05$).

C) mRNA was isolated from sh*Hif1α*, sh*Hif2α*, sh*Ahr*, and shScr stably transfected adipocytes after eight days of differentiation, and subjected to normoxia, hypoxia (0.1% O_2 for 16h), or 200 nM $CoCl_2$ for 16 hrs. Expression of *Glut1*, *Glut4*, Vegf, *Cytc1* and *Cox4.2* was measured by qPCR. Data shown as mean ± SEM of four samples and repeated twice.